NANO SCATTERING PARTICLE: AN APPROACH TO IMPROVE QUALITY OF THE COMMERCIAL LED

SỬ DỤNG HẠT TÁN XẠ NANO ĐỂ CẢI THIỆN CHẤT LƯỢNG ĐÈN LED THƯƠNG MẠI

Nguyen Doan Quoc Anh*

Ton Duc Thang University, Hochiminh, Vietnam

*Corresponding author: nguyendoanquocanh@tdtu.edu.vn

(Received: December 14, 2023; Revised: January 23, 2024; Accepted: January 29, 2024)

Abstract - The light-emitting diodes (LEDs) have emerged as a sustainable illumination solution in the lighting industry. However, the commercial LEDs suffer from low chromatic rendition performance. This work proposes a feasible approach to enhance the quality of commercial LED packages via regulating scattering factors. The TiO_2 nano scattering particles are added into the YAG:Ce^{3+} compound to enhance the internal scattering performance, inducing the blue-light conversion and extraction. In this work, TiO_2 concentration varies from 0 wt% to 20 wt%. Results show that 5 wt% of TiO_2 is the right concentration to achieve the optimal scattering performance for improvements in luminosity and color rendition of the LED. If the TiO_2 concentration is beyond 5 wt%, these two parameters decline owing to too intensive light scattering. Meanwhile, 10 wt% is the most appropriate concentration of TiO_2 to enhance the color uniformity of the LED.

Key words - Commercial LED; color rendering index; nano scattering particles; lumen output; scattering performance

Tóm tắt - Đèn LED đã và đang trở thành một giải pháp chiếu sáng bền vững trong ngành chiếu sáng. Tuy nhiên, đèn LED thương mại có hiệu suất hiển thị màu sắc thấp. Bài báo này đề xuất một cách tiếp cận khả thi nhằm nâng cao chất lượng của đèn LED thương mại thông qua việc điều chỉnh các hệ số tán xạ. Cụ thể, hạt tán xạ nano TiO_2 được thêm vào lớp phốt pho YAG:Ce^{3+} để nâng cao hiệu suất tán xạ, từ đó cải thiện sự chuyển đổi và chiết xuất ánh sáng xanh từ LED chíp. Trong nghiên cứu này, nồng độ TiO_2 thay đổi từ 0 wt% đến 20 wt%. Kết quả thu được cho thấy 5 wt% là nồng độ TiO_2 phù hợp để đạt được hiệu quả tán xạ tốt nhất cho việc cải thiện quang thông và bảo toàn chỉ số hoàn màu của đèn LED. Nếu nồng độ TiO_2 vượt quá 5 wt% thì hai thông số này sẽ suy giảm do tán xạ ánh sáng quá mạnh. Trong khi đó, 10 wt% là nồng độ TiO_2 phù hợp nhất để cải thiện đồng dạng màu của đèn LED.

Từ khóa - Đèn LED thương mại; chỉ số hoàn màu; hạt tán xạ nano; độ sáng; hiệu suất tán xạ

1. Introduction

Since the first introduction in 1962, light-emitting diodes (LEDs) have emerged as a sustainable lighting solution in the lighting industry [1-3]. LEDs demonstrate several illumination benefits, including low-energy consumption, long-term operation, better light performance, and environmental-friendly technology [4-6]. The LED model can be fabricated with various approaches, but one of the most common techniques is the use of phosphor to convert blue/ultraviolet radiation from the LED chip. Commercial LEDs utilize this technique, taking the yellow phosphor trivalent cerium-activated yttrium aluminum garnet (YAG:Ce^{3+}) to transform the blue LED chip radiation to achieve white light. Studies demonstrate the high luminescence of this package, yet the color rendition performance is inferior to traditional lighting devices [7-9]. Thus, it is essential to figure out the simple but efficient way to enhance the performance of the commercial domestic LED packages, especially in chromatic rendition.

Internal light scattering is a simple approach to regulating the lighting output of the LED device [10-12]. There are various methods to achieve better scattering performance for the LED package, for example, enhancing the surface roughness, modifying phosphor composition for more scattering centers, or coupling nano scattering particles to enhance the scattering function of the phosphor encapsulation [13, 14]. Among these methods, the last one seems to be the most feasible way to carry out and manage. The scattering can be controlled with varying concentration or particle size of the added nanoparticles [15, 16]. Among widely investigated nanoparticles, TiO_2 nanoparticles offer great scattering efficiency across the entire visible spectrum, high stability, and versatile application capabilities [17, 18]. Moreover, to the best of our knowledge, TiO_2 is barely investigated as a scattering enhancement factor for LED lighting [19-22]. Therefore, in our work, the commercial LED is produced with a commercial blue LED chip, yellow phosphor YAG: Ce^{3+}, and TiO_2 nanoparticles. The particle size of TiO_2 was constant during our examination. The doping concentration of TiO_2 was varied, by which we can investigate the scattering effects on the lighting performance of the LED package. Besides, the Mie-scattering theory was applied for the scattering computation, demonstrated in section 2. In Section 3, the obtained data are demonstrated in the graphical diagram and discussed. Shortly, the TiO_2 addition contributes to improving the lighting efficiency and color rendition performance of domestic commercial LEDs.

2. Scattering computation and LED simulation

2.1. Scattering computation

The Mie-scattering function [23-26] of spherical particles is applied to investigate the scattering factor of the TiO_2 in the phosphor layer. The calculated scattering factors include $\mu_{sc}(\lambda)$ – scattering coefficients (SC) and δ_{sc} – reduced scattering coefficients (RSC). The SC and RSC are computed using the following equations:

$$\mu_{sc}(\lambda) = \int N(r) C_{sc}(\lambda, r) dr \quad (1)$$

$$\delta_{sc} = \mu_{sc}(1 - g) \quad (2)$$

where λ, r, and g represent the wavelength (nm), the particle size of the TiO_2 (μm), and the anisotropy function, respectively. $N(r)$ and C_{sc} represent the TiO_2 distribution density and scattering cross section, correspondingly.

The anisotropy function g, $N(r)$, and C_{sc} are expressed as:

$$g = 2\pi \iint_{-1}^{1} p(\theta,\lambda,r) f(r) cos\theta d cos\theta dr \quad (3)$$

$$N(r) = N_d(r) + N_p(r) \quad (4)$$

$$C_{sc} = \frac{2\pi}{k^2}\sum_0^\infty (2n-1)(|a_n|^2 + |b_n|^2) \quad (5)$$

where in eq.(3), θ is the viewing angle, and $p(\theta,\lambda,r)$ is the phase function that is calculated with eqs. (6) and (7). In (4), $N_d(r)$ and $N_p(r)$ indicate the particle densities of the scattering particle TiO_2 and phosphor particle $YAG:Ce^{3+}$, respectively. In eq. (5), $k = 2\pi/\lambda$, a_n and b_n are reckoned with eqs. (7) and (8).

$$p(\theta,\lambda,r) = \frac{4\pi \times 1/2(|S_1(\theta)|^2 + |S_2(\theta)|^2)}{k^2 C_{sc}(\lambda,r)} \quad (6)$$

with $S_1(\theta)$ and $S_2(\theta)$ denote angular scattering amplitudes:

$$S_1(\theta) = \sum_{n-1}^{\infty} \frac{2n+1}{n(n+1)} \left[\begin{matrix} a_n(x,m)\pi_n(cos\theta) + \\ b_n(x,m)\tau_n(cos\theta) \end{matrix} \right]$$

$$S_2(\theta) = \sum_{n-1}^{\infty} \frac{2n+1}{n(n+1)} \left[\begin{matrix} a_n(x,m)\tau_n(cos\theta) + \\ b_n(x,m)\pi_n(cos\theta) \end{matrix} \right]$$

$$a_n(x,m) = \frac{\psi_n'(mx)\psi_n(x) - m\psi_n(mx)\psi_n'(x)}{\psi_n'(mx)\xi_n(x) - m\psi_n(mx)\xi_n'(x)} \quad (7)$$

$$b_n(x,m) = \frac{m\psi_n'(mx)\psi_n(x) - \psi_n(mx)\psi_n'(x)}{m\psi_n'(mx)\xi_n(x) - \psi_n(mx)\xi_n'(x)} \quad (8)$$

with $x = k.r$, m represents the refractive indices, $\psi_n(x)$ and $\xi_n(x)$ indicate Riccati-Bessel functions [27-29].

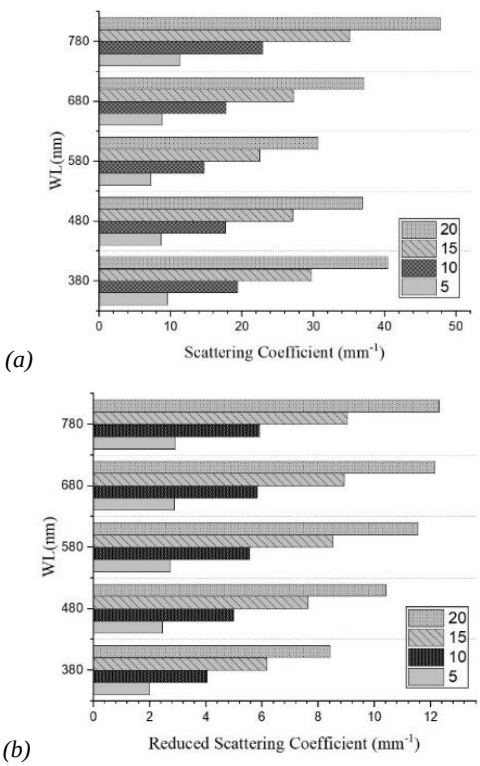

Figure 1. *Scattering factor of the phosphor compound with varying TiO_2 concentration: (a) scattering coefficients (SC) and (b) reduced scattering coefficients (RSC)*

The SC and RSC of the phosphor compound are demonstrated in Figure 1, in which Figure 1(a) is the SC data and Figure 1(b) is the RSC data. Overall, the scattering factor increases when we increase the concentration of TiO_2. When observing the scattering factors under the visible wavelength from 380 nm to 780 nm, the SC value under 780 nm wavelength (deep red) is the best while that under 580 nm (yellow-green) is the lowest. Meanwhile, the RSC value increases as the examined wavelength becomes longer. These results demonstrate the potential of using high TiO_2 concentration to induce the scattering performance at different angles.

2.2. LED simulation

Using the LightTools 9.0 software [30], combined with the Monte Carlo path-trace method, we simulated the LED package in our work, as shown in Figure 2. Specifically, Figure 2(a) is a photo of the actual LED. Figure 2(b) is a schematic diagram of a cluster of nine LED chips. Figures 2(c) and 2(d) are the simulation models of the LED that we studied. According to Mie-theory, the TiO_2 and phosphor particles have spherical shapes, with an average radius of about 3 μm and 7.25 μm, respectively.

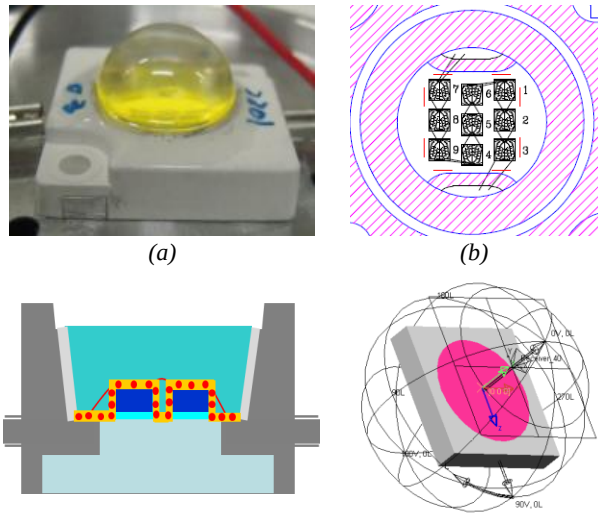

Figure 2. *LED structure simulation: (a) Actual LED, (b) Bonding diagram, (c) Illustration of pc-WLEDs model, (d) Simulation of LED using LightTools software*

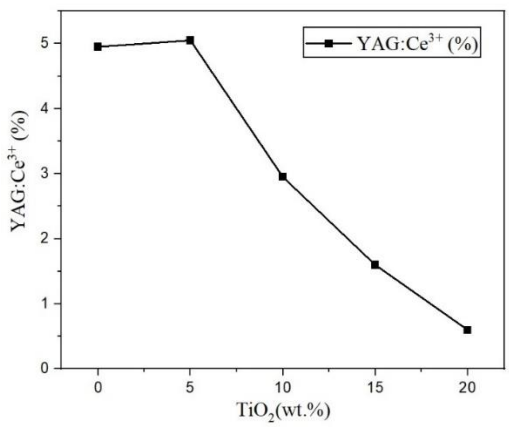

Figure 3. *$YAG:Ce^{3+}$ phosphor concentration with varying TiO_2 concentration*

The investigation focuses on the changes in the optical performance of the LED with different weight percentages of TiO_2, from 0-20 wt%. When increasing TiO_2 concentration, the yellow-phosphor YAG:Ce^{3+} doping amount must be reduced to keep the correlated color temperature (CCT) stable while hindering the self-absorption phenomenon. This inversion in their concentration can be observed in Figure 3.

3. Simulation results and discussion

3.1. Emission power and lumen intensity of LED

The emission power of the commercial LED with different TiO_2 concentrations is presented in Figure 4. In general, we observe two distinguishing emission bands: a narrow band in the blue region with a peak at 450 nm, and a broader band in the green-red region (500-595 nm) with a sharp peak at 545 nm and a shoulder peak at 575 nm. In comparison with the reference value (at 0 wt% of TiO_2), we notice that with 5 wt% of TiO_2, the intensity of the two emission bands slightly increases. However, continuing to increase the TiO_2 amount results in a significant decline in both emission band's intensity. In addition, another emission peak at about 525 nm emerges as the TiO_2 concentration reaches 15-20 wt%.

The emission peak at 450 nm can be attributed to the blue LED emission while the other peaks could be from the phosphor compound doping TiO_2 [31]. The appearance of a new peak indicates that the increasing TiO_2 concentration enhances the blue-light conversion of the phosphor compound. However, though the higher scattering performance is beneficial to blue-light utilization, it reduces the emitted light energy. When light travels through many scattering events, the energy absorption by phosphor increases, resulting in the observed lower emission intensity [32]. Consequently, the lumen output of the LED degrades.

The lumen of the LED package is depicted in Figure 5. A slight increase in lumen output is noticed when we use 5 wt% of TiO_2 in the phosphor compound. At higher concentrations, the lumen intensity declines notably. Such results are in alignment with the discussed data on the LED's emission power.

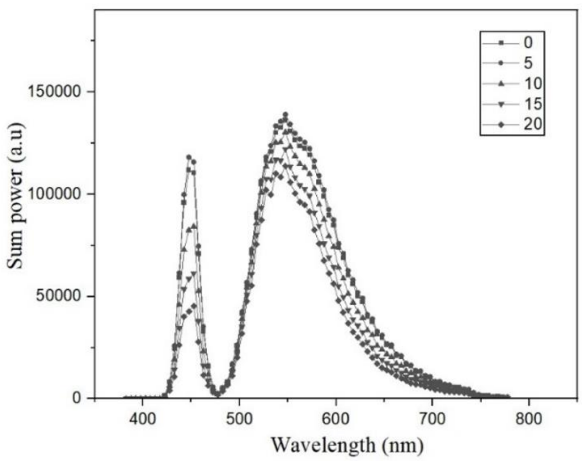

Figure 4. *Emission power of the LED with varying TiO_2 concentration*

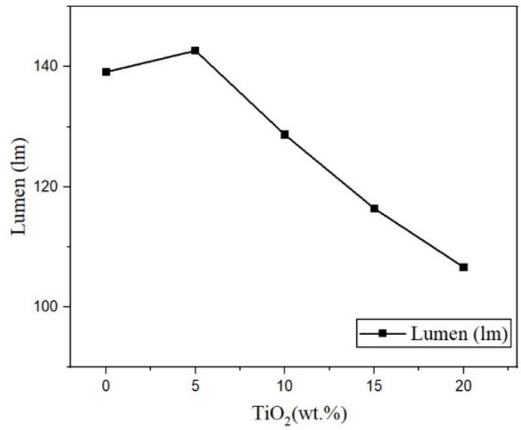

Figure 5. *Lumen output of the LED with varying TiO_2 concentration*

3.2. Color uniformity and color rendition

The scattering performance can affect the color uniformity of the white light emitted by the LED. To achieve higher color uniformity, the chroma deviation (or delta CCT) should be minimized, which can be done by enhancing the scattering performance [33]. Figure 6 shows the chroma deviation of the LED with different TiO_2 concentrations, and Figure 7 shows the corresponding angular-CCT values.

We can see a significant fluctuation in the CCT ranges with increasing TiO_2 concentration, due to the absorption and scattering effects of the phosphor materials. Within the viewing angle from 70^0 to -70^0, the highest CCT range is noted with 5 wt% of TiO_2. Meanwhilen the most stable CCT range is achievable with 10 wt% of TiO_2. This implies that using TiO_2 concentration at 10 wt% can accomplish the highest color-distribution uniformity. To confirm this, we take into consideration the color deviation. Compared with the reference sample without doping TiO_2, the 5wt% sample shows the increasing and highest D-CCT level. On the other hand, with the 10 wt% TiO_2-doped sample, the D-CCT bottoms out at below 50 K, much lower than the reference level. Therefore, we can confirm that 10 wt% TiO_2 concentration is the optimal condition to achieve the best color uniformity for the commercial LED light.

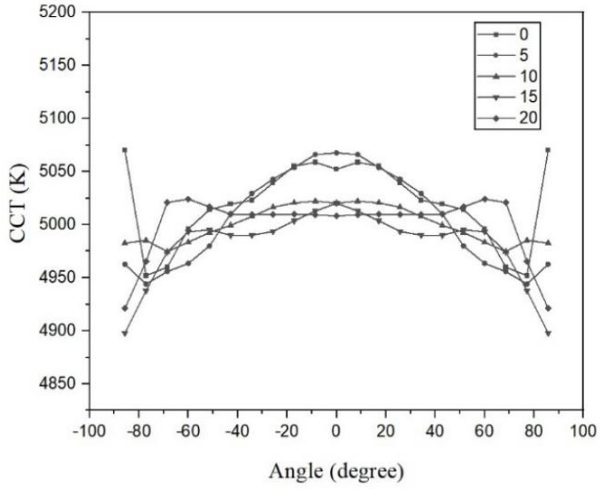

Figure 6. *CCT ranges of the LED with varying TiO_2 concentration*

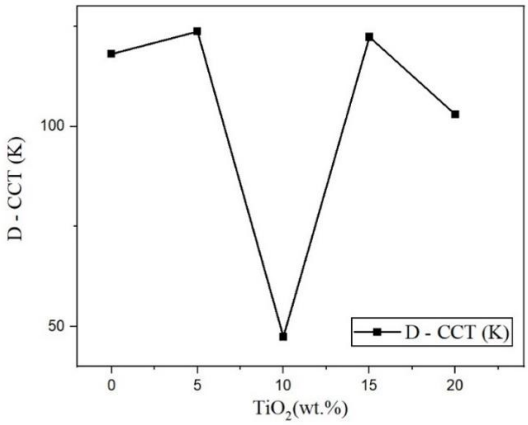

Figure 7. *Color deviation (D-CCT) of the LED with varying TiO_2 concentration*

We have also evaluated the rendering efficiency of the LED light with the TiO_2-embedded phosphor compound. Two parameters to measure the rendering efficiency for the assessment include the color rendering index (CRI) and the color quality scale (CQS). The CQS can be seen as a more comprehensive metric than the CRI, as it considers various factors such as hue preservation, chroma enhancement, gamut area index, and gamut shape index. The CQS can provide a more detailed and accurate assessment of the color performance of a light source, which is useful for optimization in different applications [34-36].

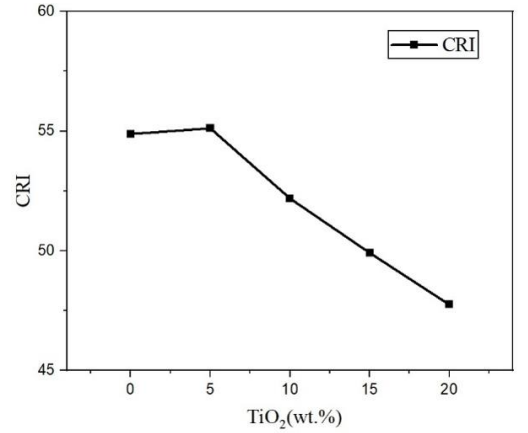

Figure 8. *CRI levels of the LED with varying TiO_2 concentration*

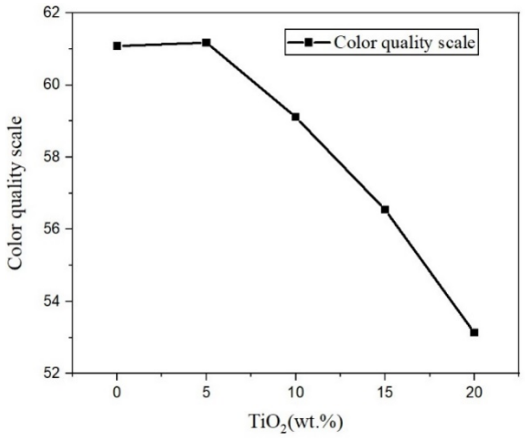

Figure 9. *CQS levels of the LED with varying TiO_2 concentration*

Figure 8 shows the CRI values while Figure 9 depicts the CQS values of the LED light with different TiO_2 concentrations. The results were obtained by employing LightTools software to simulate the CRI and CQS trends when adjusting the TiO_2 amounts from 0 wt% to 20 wt%. It is possible to observe a slight increase in both CQS and CRI levels when the concentration of TiO_2 increases from 0 wt% to 5 wt%. However, the higher concentration numbers of TiO_2 initiate the decline in CRI and CQS. Such declines become more significant when the TiO_2 amount further increases. This can be attributed to the lack of blue color intensity while the yellow-green color range is dominant. Such imbalance in color is induced by the intensive scattering, leading to a high conversion of blue to yellow-green, with high TiO_2 concentration. Thus, if we need to improve the luminosity and color reproduction performance, 5 wt% of TiO_2 is a suitable concentration since the scattering strength is not too intensive to diminish the incident light transmission power. Meanwhile, if we focus on achieving better color uniformity, 10 wt% of TiO_2 is recommended.

4. Conclusion

This paper has presented a novel method to improve the quality of commercial LED packages by controlling the scattering factors. TiO_2 nano scattering particles are embedded into the YAG:Ce^{3+} compound to increase the internal scattering performance, which enhances the blue-light conversion and extraction. We have measured the luminosity and color rendition of the LED with different TiO_2 concentrations ranging from 0 wt% to 20 wt%. From the results, we have found that 5 wt% of TiO_2 is the optimal concentration to achieve the improvements in CRI and CQS, as well as the lumen output of the LED. In addition, 10 wt% is the best TiO_2 amount to achieve the lowest color deviation or the most enhanced color uniformity distribution. However, beyond such levels, the lumen and color rendition decrease due to excessive light scattering.

REFERENCES

[1] L. Xu, Q. Ye, and M. R. Luo, "Estimation of the perceptual color gamut on displays", *Optics Express*, vol. 30, no. 24, pp. 43872-43887, 2022. https://doi.org/10.1364/OE.472808.

[2] S. Zhang, J. Y. Xin Cheng, J. J. Chua, X. Li, and M. Olivo, "Dual-modality hyperspectral microscopy for transmission and fluorescence imaging", *Optics Continuum*, vol. 1, no. 11, pp. 2404-2415, 2022. https://doi.org/10.1364/optcon.469040.

[3] P. Tinning, M. Donnachie, J. Christopher, D. Uttamchandani, and R. Bauer, "Miniaturized structured illumination microscopy using two 3-axis MEMS micromirrors", *Biomedical Optics Express*, vol. 13, no. 12, pp. 6443-6456, 2022. https://doi.org/10.1364/boe.475811.

[4] S.-M. Lee, J.-W. Jung, and Y.-J. Kim, "Design and evaluation of thermally conductive sheet structure to enhance the thermal stability of transparent OLED displays", *Journal of the Optical Society of America B*, vol. 39, no. 12, pp. 3216-3222, 2022. https://doi.org/10.1364/josab.474776.

[5] X. Dai *et al.*, "Detection band expansion by independently tunable double resonances in a long-wavelength dual-color QWIP", *Optics Express*, vol. 30, no. 24, pp. 43579-43589, 2022. https://doi.org/10.1364/oe.472051.

[6] B. Karadza, H. V. Avermaet, L. Mingabudinova, Z. Hens, and Y. Meuret, "Comparison of different RGB InP-quantum-dot-on-chip

LED configurations", *Optics Express*, vol. 30, no. 24, pp. 43522-43533, 2022. https://doi.org/10.1364/oe.476135.

[7] Y. Gao and L. Cao, "Projected refractive index framework for multi-wavelength phase retrieval", *Optics Letters*, vol. 47, no. 22, pp. 5965-5968, 2022. https://doi.org/10.1364/ol.476707.

[8] S. Na, S. Kim, J. Lee, Y. Kim, and H. Kim, "Design of a three-phase amplitude macro-pixel full-color complex spatial light modulator with an in-cell geometric phase retardation layer", *Optics Letters*, vol. 47, no. 22, pp. 5909-5912, 2022. https://doi.org/10.1364/ol.475087.

[9] G. E. Rizaev, L. V. Seleznev, D. V. Mokrousova, D. V. Pushkarev, and A. A. Ionin, "Terahertz emission pattern from a single-color filament plasma", *Optics Letters*, vol. 47, no. 22, pp. 5917-5920, 2022. https://doi.org/10.1364/ol.476382.

[10] M. Guttmann *et al.*, "Light extraction efficiency and internal quantum efficiency of fully UVC-transparent AlGaN based LEDs", *Journal of Physics D: Applied Physics*, vol. 54, no. 33, p. 335101, 2021. https://doi.org/10.1088/1361-6463/ac021a.

[11] K. L. Tsakmakidis, "Scattered light for white LEDs", *Nature Materials*, vol. 12, no. 6, p. 472, 2013. https://doi.org/10.1038/nmat3677.

[12] K. Lee *et al.*, "A light scattering layer for internal light extraction of organic Light-Emitting diodes based on silver nanowires", *ACS Applied Materials & Interfaces*, vol. 8, no. 27, pp. 17409-17415, 2016, https://doi.org/10.1021/acsami.6b02924.

[13] D. R. Smith, S. Shivkumar, J. Field, J. W. Wilson, H. Rigneault, and R. A. Bartels, "Nearly degenerate two-color impulsive coherent Raman hyperspectral imaging", *Optics Letters*, vol. 47, no. 22, pp. 5841-5844, 2022. https://doi.org/10.1364/OL.467970.

[14] Y. Wang *et al.*, "Highly sensitive multi-stage terahertz parametric upconversion detection based on a KTiOPO4 crystal", *Optics Letters*, vol. 47, no. 22, pp. 5853-5856, 2022. https://doi.org/10.1364/OL.473955.

[15] M. Polché, B. F. J. Miguel, C. A. G. González, G. Gonzalez-Contreras, and V. H. R. Arellano, "Study of the Scattering Effect by SiO2 Nanoparticles, in a Luminescent Solar Concentrator Sensitized with Carbon Dots", *Nanomaterials*, vol. 13, no. 17, p. 2480, 2023. https://doi.org/10.3390/nano13172480.

[16] C.-H. Shin, E. Y. Shin, M. Kim, J.-H. Lee, and Y. Choi, "Nanoparticle scattering layer for improving light extraction efficiency of organic light emitting diodes", *Optics Express*, vol. 23, no. 3, pp. A133-A139, 2015. https://doi.org/10.1364/OE.23.00A133.

[17] M. Tsega and F. B. Dejene, "Morphological, thermal and optical properties of TiO2 nanoparticles: The effect of titania precursor", *Materials Research Express*, vol. 6, no. 6, p. 065041, 2019. https://doi.org/10.1088/2053-1591/ab0dd3.

[18] Y. Désières, D.-Y. Chen, D. Visser, C. F. Schippers, and S. Anand, "Strong light extraction enhancement using TiO2 nanoparticles-based microcone arrays embossed on III-Nitride light emitting diodes", *Applied Physics Letters*, vol. 112, no. 23, p. 231101, 2018. https://doi.org/10.1063/1.5021301.

[19] T.-H. Tsai, Z. Wang, and H. Takahashi, "Reversible photochromic effect in natural gemstone sapphires", *Optics Letters*, vol. 47, no. 22, pp. 5805-5808, 2022. https://doi.org/10.1364/ol.474838.

[20] K. He *et al.*, "Blue and white light modulation of a flexible electroluminescent device based on phosphors", *Optics Letters*, vol. 47, no. 22, pp. 5770-5772, 2022. https://doi.org/10.1364/ol.474838.

[21] A. A. Silaev, A. A. Romanov, and N. V. Vvedenskii, "Multicolor and supercontinuum radiation generation in terahertz and mid-infrared ranges due to the gas ionization by two-color chirped laser pulses", *Journal of the Optical Society of America B*, vol. 40, no. 1, pp. A28-A35, 2022. https://doi.org/10.1364/josab.469750.

[22] C.-H. Chuang, C.-Y. Chen, S.-T. Li, H.-T. Chang, and H.-Y. Lin, "Miniaturization and image optimization of a full-color holographic display system using a vibrating light guide", *Optics Express*, vol. 30, no. 23, pp. 42129-42140, 2022. https://doi.org/10.1364/oe.473150.

[23] J. Bak, R. Randolph, and A. Gerakis, "Dual color, frequency, pulse duration and shape agile laser system for particle spectroscopy and manipulation", *Optics Express*, vol. 30, no. 23, pp. 41709-41723, 2022. https://doi.org/10.1364/oe.470764.

[24] P. Lv *et al.*, "Solution-processed electroluminescent white-light-emitting devices based on AIE molecules and Cu-In-Zn-S nanocrystals", *Photonics Research*, vol. 10, no. 11, pp. 2622-2627, 2022. https://doi.org/10.1364/prj.472419.

[25] K. J. Turner, M. Tzortziou, B. K. Grunert, J. Goes, and J. Sherman, "Optical classification of an urbanized estuary using hyperspectral remote sensing reflectance", *Optics Express*, vol. 30, no. 23, pp. 41590-41612, 2022. https://doi.org/10.1364/oe.472765.

[26] K. Chen, W. Li, and K. Xu, "Super-multiplexing excitation spectral microscopy with multiple fluorescence bands", *Biomedical Optics Express*, vol. 13, no. 11, pp. 6048-6060, 2022. https://doi.org/10.1364/boe.473241.

[27] M. V. Berry, "Caustic of colors in Newton's prism", *Journal of the Optical Society of America A*, vol. 39, no. 12, pp. C45-C50, 2022. https://doi.org/10.1364/josaa.474473.

[28] X. Peng, Y. Shi, Z. Ren, and Y. Ying, "Practical method for dynamic color holographic display", *Applied Optics*, vol. 61, no. 31, pp. 9198-9202, 2022. https://doi.org/10.1364/ao.471751.

[29] M. Lecca, G. Gianini, and R. P. Serapioni, "Mathematical insights into the original Retinex algorithm for image enhancement", *Journal of the Optical Society of America A*, vol. 39, no. 11, pp. 2063-2072, 2022. https://doi.org/10.1364/josaa.471953.

[30] M. Gesley and R. Puri, "Rendering spectral images", *Journal of the Optical Society of America A*, vol. 39, no. 11, pp. 2035-2044, 2022. https://doi.org/10.1364/josaa.470814.

[31] D. Luo, L. Wang, S. W. Or, H. Zhang, and R. Xie, "Realizing superior white LEDs with both high R9 and luminous efficacy by using dual red phosphors", *RSC Advances*, vol. 7, no. 42, pp. 25964–25968, 2017. https://doi.org/10.1039/c7ra04614f.

[32] V. Leung, A. Lagendijk, T. Tukker, A. Mosk, W. L. IJzerman, and W. L. Vos, "Interplay between multiple scattering, emission, and absorption of light in the phosphor of a white light-emitting diode", *Optics Express*, vol. 22, no. 7, pp. 8190-8204, 2014. https://doi.org/10.1364/OE.22.008190.

[33] P. -C. Wang, Y. -K. Su, C. -L. Lin and G. -S. Huang, "Improving Performance and Reducing Amount of Phosphor Required in Packaging of White LEDs With TiO_2 -Doped Silicone", *IEEE Electron Device Letters*, vol. 35, no. 6, pp. 657-659, 2014. https://doi.org/10.1109/led.2014.2318037.

[34] Z. Yu *et al.*, "High-performance full-color imaging system based on end-to-end joint optimization of computer-generated holography and metalens", *Optics Express*, vol. 30, no. 22, pp. 40871-40883, 2022. https://doi.org/10.1364/oe.470419.

[35] P. Sang *et al.*, "Al_2O_3-YAG:Ce/YAG composite ceramic phosphor in a transmissive configuration for high-brightness laser-driven lighting", *Optics Express*, vol. 30, no. 22, pp. 40951-40964, 2022. https://doi.org/10.1364/oe.475226.

[36] A. X. Desai, G. R. Schmidt, and D. T. Moore, "Achromatization of multi-material gradient-index singlets", *Optics Express*, vol. 30, no. 22, pp. 40306-40314, 2022. https://doi.org/10.1364/oe.470380.